Original article

Synthesis of novel nano-radiotracer for in-vivo molecular SPECT imaging: Nanosize chitosan and its conjugation with glutamine

Manyan Nejati [a], Morteza Pirali Hamedani [a,d], Seyed Esmaeil Sadat Ebrahimi [a,d], Mostafa saffari [b], Mehdi Shafiee Ardestani [a,*], Seyedeh Masoumeh Ghoreishi [c,*]

[a] Department of Radiopharmacy, Faculty of Pharmacy, Tehran University of Medical Sciences, Tehran, Iran
[b] Department of Pharmaceutics & Medical Nanotechnology, Branch of Pharmaceutical Sciences, Islamic Azad University, Tehran, Iran
[c] Cellular and Molecular Biology Research Center, Health Research Institute, Babol University of Medical Sciences, Babol, Iran
[d] Department of Medicinal Chemistry, Faculty of Pharmacy, Tehran University of Medical Sciences, Tehran, Iran

ARTICLE INFO

ABSTRACT

This study presents the synthesis and characterization of chitosan-glutamine-based biocompatible nanoparticles (nano-conjugate) as a platform for developing an efficient nano-radiopharmaceutical agent for liver imaging. The nanoparticles were labeled with technetium-99 m, resulting in the formation of ^{99m}Tc-chitosan-glutamine. Various characterization techniques, including furrier transform infrared spectroscopy (FT-IR) and proton nuclear magnetic resonance (^{1}H NMR) were performed for confirmation of synthesized nano-conjugate. Scanning electron microscopy (SEM), dynamic light scattering (DLS), and static light scattering (SLS) spectroscopies were employed to investigate the particle properties such as size, zeta potential, and molecular weight. MTT assay was conducted to study the toxicity of chitosan-glutamine showing that nano-conjugate had a toxicity on cancer cell in-vitro. In-vivo studies were conducted by administering ^{99m}Tc-chitosan-glutamine to mice, followed by whole body SPECT imaging. The imaging process was performed at three different time points post-injection: 15, 60, and 120 min. The SPECT results revealed a significantly accumulation in the liver. Also, biodistribution study showed that accumulation in liver (% ID/g = 23.15%) was significantly higher than other organs. Our in-vitro and in-vivo findings suggest that ^{99m}Tc-chitosan-glutamine could serve as a theranostic agent for cancer imaging using SPECT technology.

1. Introduction

For years, nanotechnology has fascinated researchers due to its applications in wide variety of fields, including biosensors, medical and pharmaceutical science, catalysis, engineering and so on. Today, nanotechnology has been entered widely in the development of pharmaceutical products. The application of nanotechnology in radiopharmaceuticals can bring about extensive changes in nuclear medicine. In recent times, nano-radiopharmacology has emerged as a significant area of focus in the fields of molecular imaging and cancer therapy. It has gained particular attention for its applications in pancreatic and stromal tumors, as well as renal cell carcinoma (de Souza Albernaz et al., 2012; Silindir-Gunay and Ozer 2017). Although several advantages have been reported for nuclear radiotherapy, numerous problems with utilizing multi-modal imaging platforms, providing targeted delivery and developing new theranostic agents are attracting the researchers (Kleynhans et al., 2018). Therefore, the development and introduction of new radiopharmaceutical agents are crucial in enhancing nuclear medicine and diagnosis of diseases (Braga 2015).

Nanoparticles offer significant advantages in various aspects of drug delivery. They have the potential to enhance the solubility of poorly water-soluble drugs, improve drug stability, and prolong the biological half-life of drugs. Additionally, nanoparticles enable targeted delivery of drugs to specific tissues or cells, allowing for more precise and effective treatment. Moreover, they can be utilized for carrying large macromolecular drugs, facilitating the simultaneous delivery of multiple drugs, and enabling visualiza-

* Corresponding authors.
E-mail addresses: shafieeardestani@gmail.com (M.S. Ardestani), s.masoumeh.gh@gmail.com (S.M. Ghoreishi).
Peer review under responsibility of King Saud University.

M. Nejati, M.P. Hamedani, Seyed Esmaeil Sadat Ebrahimi et al.

Arabian Journal of Chemistry 16 (2023) 105284

tion of target tissues in imaging. Furthermore, nanoparticles have the potential for in-vivo real-time applications, making them highly versatile and valuable in the field of biomedical research and drug development (Albernaz Mde et al., 2014; Eroglu and Yenilmez 2016; Silindir-Gunay and Ozer 2017; Kleynhans et al., 2018; Ebrahimzadeh et al., 2021; Hashemi et al., 2022a, 2022b). Radiolabeling nanoparticles with various radionuclides such as ^{11}C, ^{18}F, ^{47}Ca, ^{51}Cr, ^{62}Cu, ^{82}Rb, ^{68}Ga, ^{90}Y, ^{99m}Tc, ^{111}In, ^{131}I, ^{177}Lu allows them to be used in nuclear medicine imaging (Eberlein et al., 2011; Lopci et al., 2014; Enrique et al., 2015; Ferro-Flores et al., 2015; Janssen et al., 2016; Kleynhans et al., 2018).

A great deal of research has reported labeled nanoparticles as nano-radiopharmaceutical tracers. In this framework, ^{177}Lu-gold nanoparticle have been described for targeting molecular recognition, ^{18}F-Europium oxide (Eu$_2$O$_3$) for fluorescence molecular imaging, ^{255}Ac-Titanium oxide for alpha radionuclide therapy, ^{131}I-graphene oxide for photo-thermal therapy, ^{125}I-gold nanorods for specific inflammation imaging, ^{99m}Tc-mesoporous silica for inflammation imaging, ^{99m}Tc-RGD-polyethyleneimine for hepatic carcinoma imaging, ^{99m}Tc-chitosan for lung pharmacokinetic, and ^{99m}Tc-glutamic acid for cancer targeting imaging (Kakkar et al., 2010; Shao et al., 2011; Chen et al., 2015; Ferro-Flores et al., 2015; Hu et al., 2015; Cędrowska et al., 2018; Paul et al., 2018; Zhou et al., 2018). The use of the radioactive isotope technetium-99 m in medical applications has been extensively researched due to its specific characteristic such as pure gamma radiation, suitable half-life, and easy accessibility. Technetium-99 m commonly is employed as a radiopharmaceutical agent, and its various derivatives have demonstrated successful applications in the wide range of diagnostic imaging procedures (Eberlein et al., 2011; Braga 2015; Eroglu and Yenilmez 2016).

Among various nanomaterials, chitosan, a biocompatible and biodegradable natural polysaccharide is widely applied in biomedical applications (Choi et al., 2015). Recent studies have shown that using chitosan nanoparticles with unique physicochemical properties as radiopharmaceutical substrate can be an alternative choice due to their ability to be functionalized with biomolecules, gain high affinity toward tumor cell membrane, and overcome the drug resistance (Unsoy et al., 2014; Yhee et al., 2015; Rudzinski et al., 2016). In this case, [^{99m}Tc]Tilmanocept is a FDA approved nano-radiopharmaceuticals for lymphatic mapping which is based on chitosan targeted with mannose for solid tumors imaging in clinics (Surasi et al., 2015).

Additionally, chitosan functional groups are rich in lone pair electrons (amine and hydroxide) that could form complexes with technetium-99 m radionuclide. Many studies reported that radio-labeled ^{99m}Tc-chitosan nanoparticles have been developed for the targeted-tumor imaging for diagnosis of cancer cells at early stage (Rasaneh and Johari-Daha 2015; Othman et al., 2016; Zhang et al., 2017). Published article claimed that biocompatible amino acid (L-glutamine) has been used for the carrier systems due to its favorable surface characteristics which are very desirable for radiolabeling with three active sites (N—H, —NH$_2$ and C=O) for guest radionuclides (Dunphy et al., 2018).

In this study, low-cost chitosan-glutamine nanoparticles were prepared and labelled with technetium-99m for liver imaging. Radiochemical purity yield demonstrated that chitosan-glutamine is very favorable for forming the complex with technetium-99m radionuclide. Sulfur, nitrogen, and oxygen functional groups in the chelator's structure possess electron-rich properties which may facilitate effective binding with guest radionuclides. The presence of lone pair electrons in the nitrogen and oxygen functional groups of L-glutamine likely contribute to its suitability for complex formation with technetium-99m (Hjelstuen 1995; Taggart et al., 2016; Sakr et al., 2018). Although further studies needed to understand and investigate all properties

of ^{99m}Tc-chitosan-glutamine, our finding showed that ^{99m}Tc-chitosan-glutamine have a potential to be developed as a nano-radiopharmaceutical specifically for liver imaging, given its characteristics and biomedical features.

2. Material and method

2.1. Chemicals and reagents

Analytical-grade chemical reagents were employed without any additional purification. Isopropanol, dimethylformamide (DMF), aceton, methanol, calcium chloride (CaCl$_2$), sodium hydroxide (NaOH), Tin (II) chloride (SnCl$_2$), hydrochloric acid (HCl), ascorbic acid (vitamin C) were purchased from Merck chemical (Darmstadt, Germany). Chitosan and L-glutamine were obtained from Sigma-Aldrich (St.Louis, MO). Thermo-AVATRA FT-IR spectroscopy was used for surface functional groups of the prepared nano-conjugate. MTT powder were purchase from Sigma Aldrich. The cancerous cell line Hep-G$_2$ was gotten from the Pasteur Institute (Tehran, Iran). Fourier transform infrared spectra (FT-IR) of the powders acquired using Perkin Elmer Spectrum BX-II spectrometer. ^{1}H NMR spectra was analyzed in D$_2$O by a Bruker 500 MHz instrument. Dynamic light scattering (DLS) was measured by Malvern nano-zs. Static light scattering (SLS) technique was performed using Zetasizer ZSP (Nano-ZSP, Malvern, UK) instrument Surface morphology of the nano-conjugate was studied with TESCAN MIRA3 field emission scanning electron microscopy (Czech). AFM analysis was performed by JPK Nanowizard II. All studies were repeated three times. Research investigations were conducted in accordance with the guidelines set forth by the Tehran University of Medical Sciences, as stated in declaration IR.TUMS.PSRC. REC.1395.1333.

2.2. Synthesis of chitosan-glutamine nano-conjugate

Briefly, chitosan (30 mg) was added to the mixture of CaCl$_2$ (0.5 mL), DMF (5 mL), and EDC (300 mg) in a caped flask and stirred for 5 min at 400 rpm. After addition of L-Glutamine (2.5 mL) the mixture was stirred at 500 rpm for 1 week in a dark place at room temperature. Then, purification was done by using a dialysis bag with excess distilled water and the obtained nanoparticles were lyophilized.

2.3. Evaluation of cytotoxicity of chitosan-glutamine nano-conjugate

Cytotoxicity evaluation of chitosan-glutamine was carried out by MTT colorimetric method. In this method, a 96-well cell culture plate was used for cell seeding, and 100 μL of the media containing 10^4 cells were added to each well. Then, after appropriate treatments of chitosan-glutamine, 20 μL of media was withdrawn after 24 h, and 20 μL of MTT solution (5 mg/mL) was added into each well. The plate was incubated for 4 h in a dark place. Subsequently, the media from each well was removed and replaced with DMSO (dimethyl sulfoxide). The absorption of the samples was measured at a wavelength of 570 nm using an ELISA reader.

$$Cell survival rate = (Absorbance of test sample / Absorbance of control) \times 100$$

2.4. Labeling of chitosan-glutamine with technetium-99 m and determination of radiochemical purity

The labelling process was done by following method. Briefly, 1 mg of SnCl$_2$ was dissolved in 1 mL of hydrochloric acid (10%),
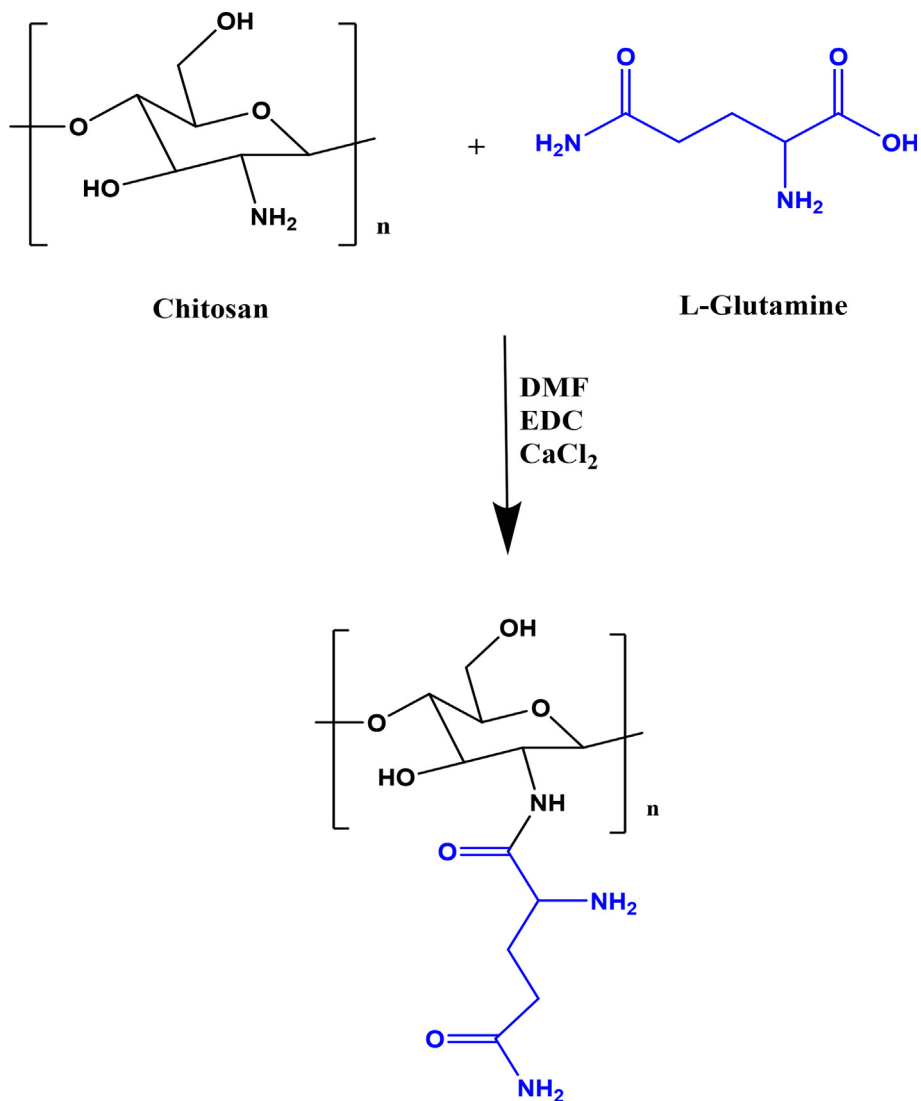
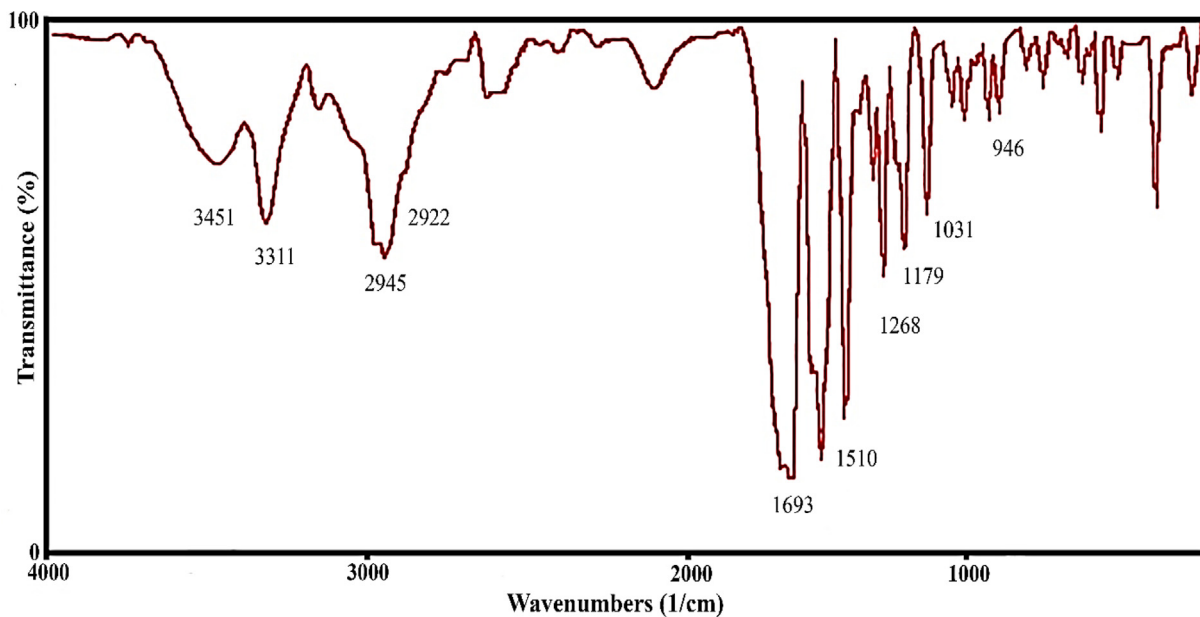**Fig. 1.** Schematic illustration for synthesis of chitosan-glutamine nano-conjugate.

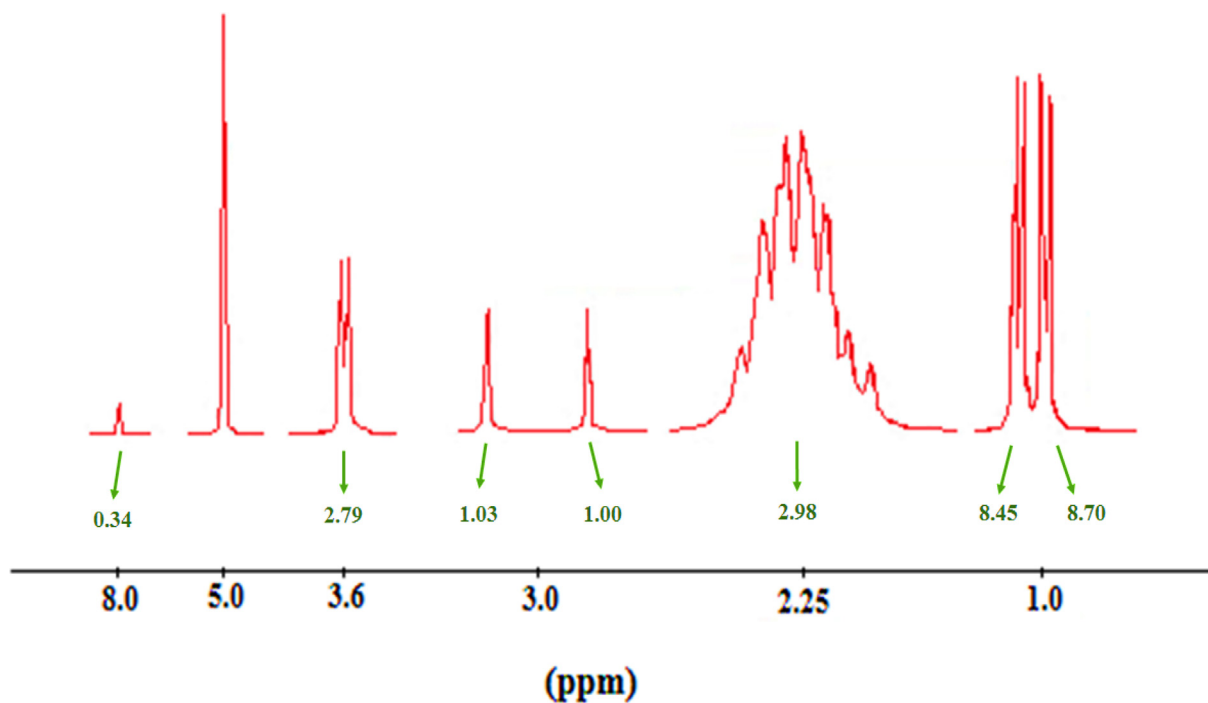**Fig. 2.** FT-IR spectra of the chitosan-glutamine nano-conjugate.
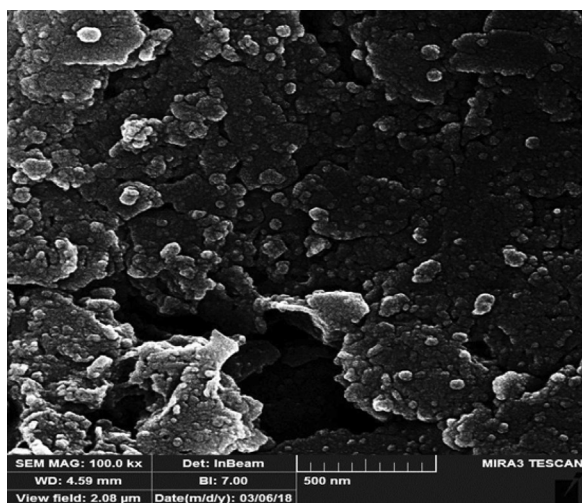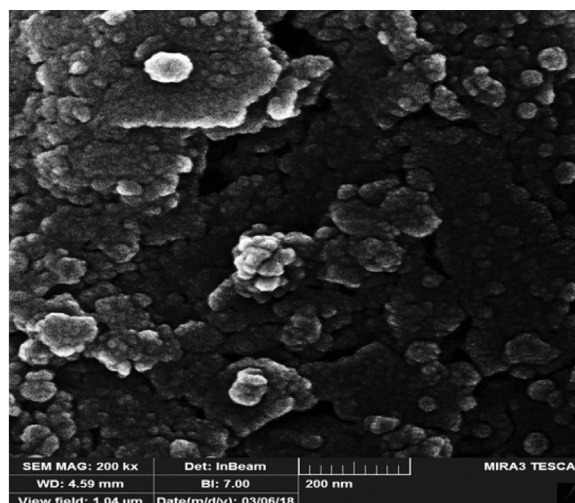
Fig. 3. ^{1}H NMR analysis of chitosan-glutamine nano-conjugate.

(A) Mag. 100 kX   **(B) Mag. 200 kX**

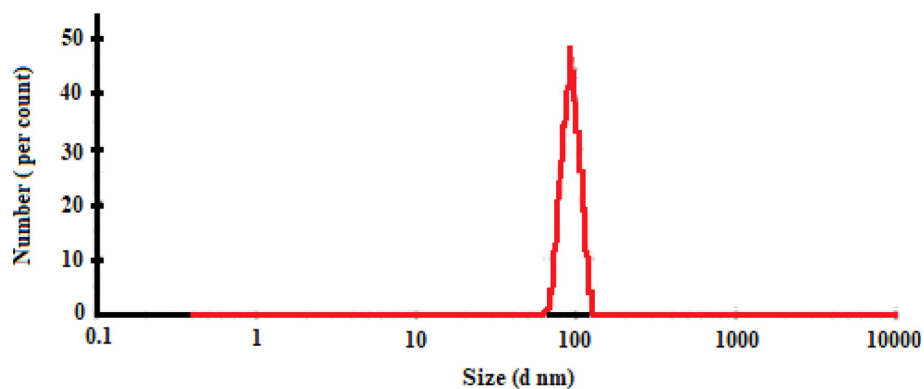**Fig. 4.** FESEM micrograph of the synthesized chitosan-glutamine nano-conjugate.

Fig. 5. Size distribution of the chitosan-glutamine nano-conjugate.

M. Nejati, M.P. Hamedani, Seyed Esmaeil Sadat Ebrahimi et al.

Arabian Journal of Chemistry 16 (2023) 105284

and 0.3 mL of the resulting solution was transferred into the vial containing chitosan-glutamine (10 mg/ml) and vitamin C powder (3 mg/ml). The pH of the solution was adjusted to 7 with 0.1 M NaOH solution and then lyophilized. Subsequently, 10 mL of freshly prepared pertechnetate ($^{99m}TcO_4^-$) solution obtained from a generator was added to the mixture and was shaken for
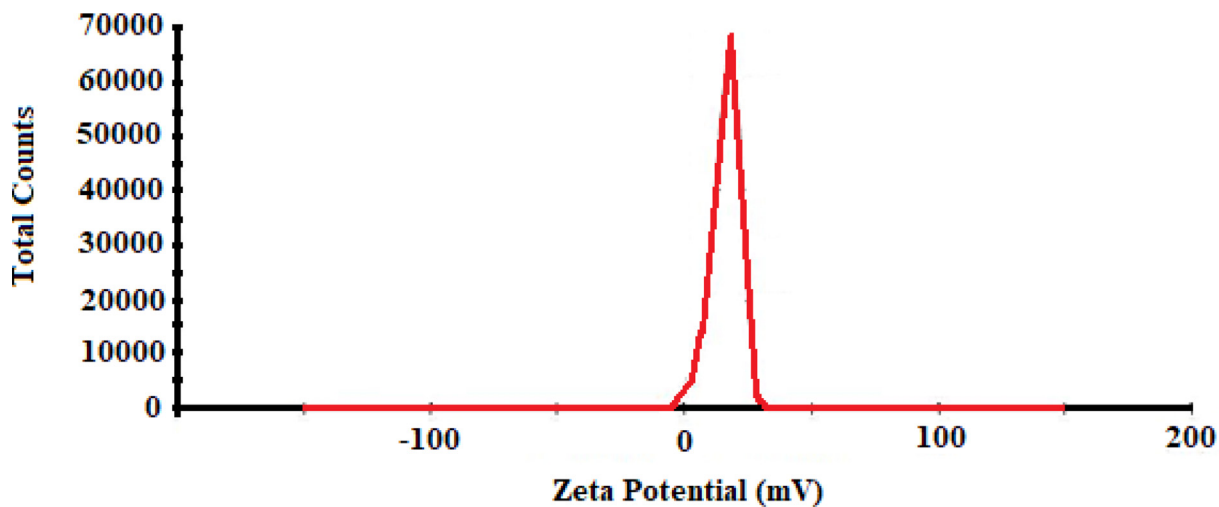

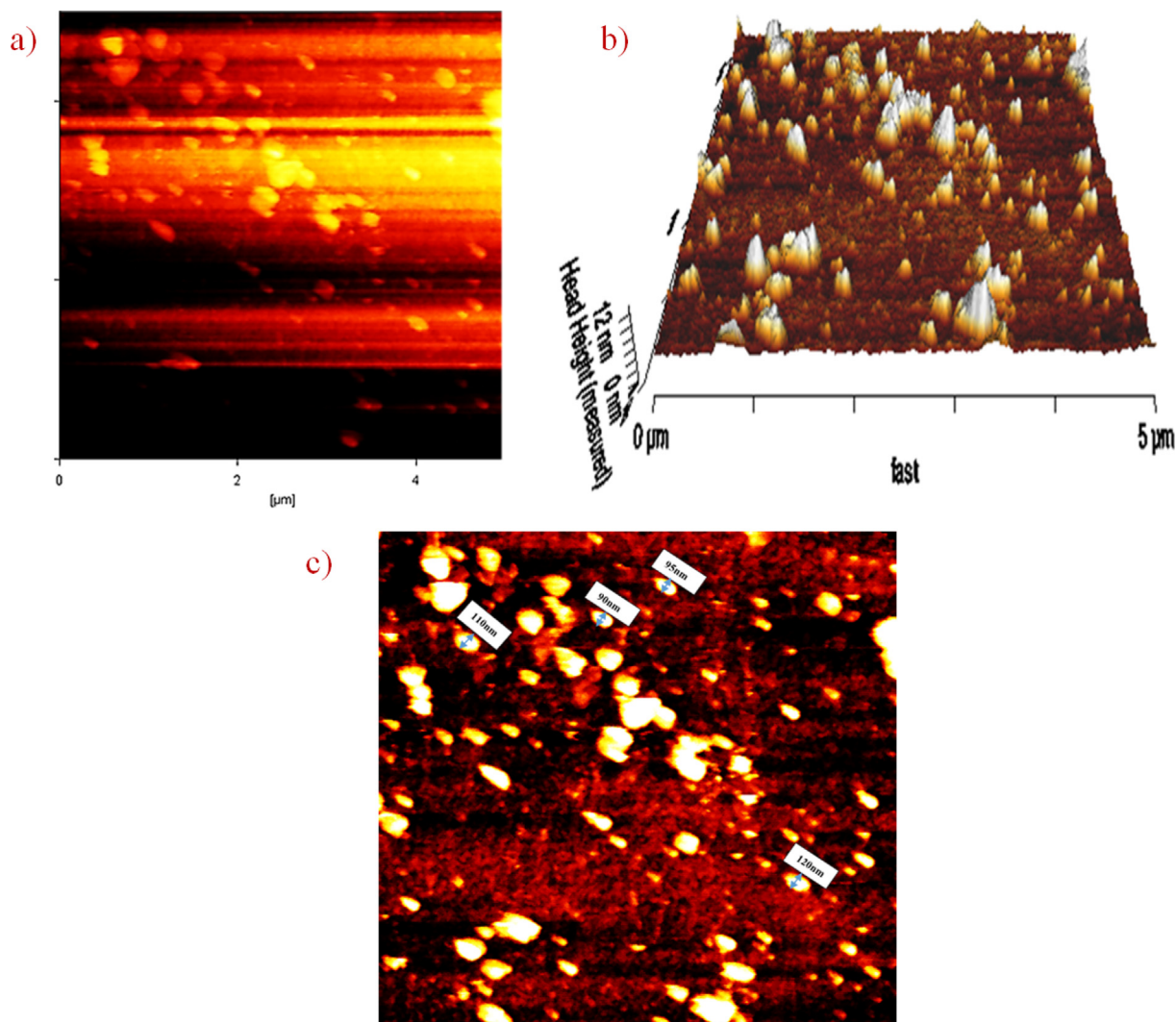Fig. 6. Zeta potential graph of chitosan-glutamine nano-conjugate.

Fig. 7. AFM micrograph of chitosan-glutamine nanoparticles; (a) two-dimensional, (b) three dimensional and (c) size of nano-conjugate.

M. Nejati, M.P. Hamedani, Seyed Esmaeil Sadat Ebrahimi et al.

Arabian Journal of Chemistry 16 (2023) 105284

20 min. Finally, the labeled material, ^{99m}Tc–chitosan-glutamine, was injected into mice through the tail vein for in-vivo investigation.

The radiochemical purity (RCP) was determined using a rapid and simple method, as described in our previous study (Ghoreishi et al., 2018). Chromatography was utilized to determine the RCP of the radio-labeled ^{99m}Tc-chitosan-glutamine. This method was chosen to save time compared to more time-consuming experiments (Amin et al., 1997). The mobile phase consisted of acetone/methanol (1:1) and saline, while Whatman paper served as the solid phase. To perform the experiment, 5 μL samples were spotted at the origin of a 1.2 cm × 10 cm paper strip. The strip was then developed in the solvent, and subsequently cut into two parts. The radioactivity in each part was measured using a gamma well-type counter. When acetone/methanol was used as the mobile phase, ^{99m}TcO$_2$ and ^{99m}Tc-chitosan-glutamine remained at the origin, while free pertechnetate migrated with the solvent. The percentage of free pertechnetate was determined based on this migration. On the other hand, when saline was used as the mobile phase, ^{99m}TcO$_2$ remained at the origin, while both free pertechnetate and ^{99m}Tc-chitosan-glutamine moved with the solvent. The amount of ^{99m}TcO$_2$ (as a percentage) was then calculated.

Finally, the radiochemical purity was evaluated using the following formula:

$$RCP = 100 - (\text{free pertechnetate} + {}^{99m}TcO_2)$$

2.5. Injection of the labeled material ^{99m} TC-chitosan-glutamine and imaging with SPECT technique

The mice were anesthetized with ketamine/xylazine and 0.5 mL (1.4 mCi) of labeled material was injected through the tail vein using insulin syringe. The mice were positioned in a supine position under the SPECT instrument and the whole-body scans were taken by imaging at different time points (15, 60, and 120 min). After imaging, the mice were killed at time 120-minute corresponding to ethical codes of working with laboratory animals. Then, in a suitable environment and with assistance of an appropriate tool the desired organs such as liver, kidney, lung, heart, brain, spleen, intestine, and bladder were separated. Thereafter, the radioactivity accumulation in each organ was measured using dose-calibrator instrument and weight of organs was recorded by digital laboratory balance. Finally, the biodistribution of each organ was calculated per gram of each organ in form of mean ± standard deviation (%ID/g).

2.6. Statistical analysis

Statistical data analysis was done using Prism 5 and excels software (Microsoft Office 2013). For quantitative data analysis One Way ANOVA followed by Tukey's test was applied. $P < 0.05$ was considered statistically significant.

3. Results and discussion

Currently, nanotechnology has gained significant attraction in the improvement of pharmaceutical science (Ebrahimzadeh et al., 2021, Hashemi et al., 2022a, 2022b). The use of nanotechnology in radiopharmaceutical science has the potential to create a huge revolution in the nuclear medicine. In our pervious study the citric acid dendrimer labelled with technetium-99 m and conjugated with glutamine was reported. Our data showed that tumor region was clearly visible with the radio-tracer (Ghoreishi et al., 2018). In this study, we aimed to design nano-radiotracer for liver imaging. For this purpose, chitosan was chosen as nano-platform capable of binding to technetium-99 m and it was conjugated with glutamine as a targeting agent. At first, chitosan-glutamine nano-conjugate synthesized as described in material and method section. Fig. 1
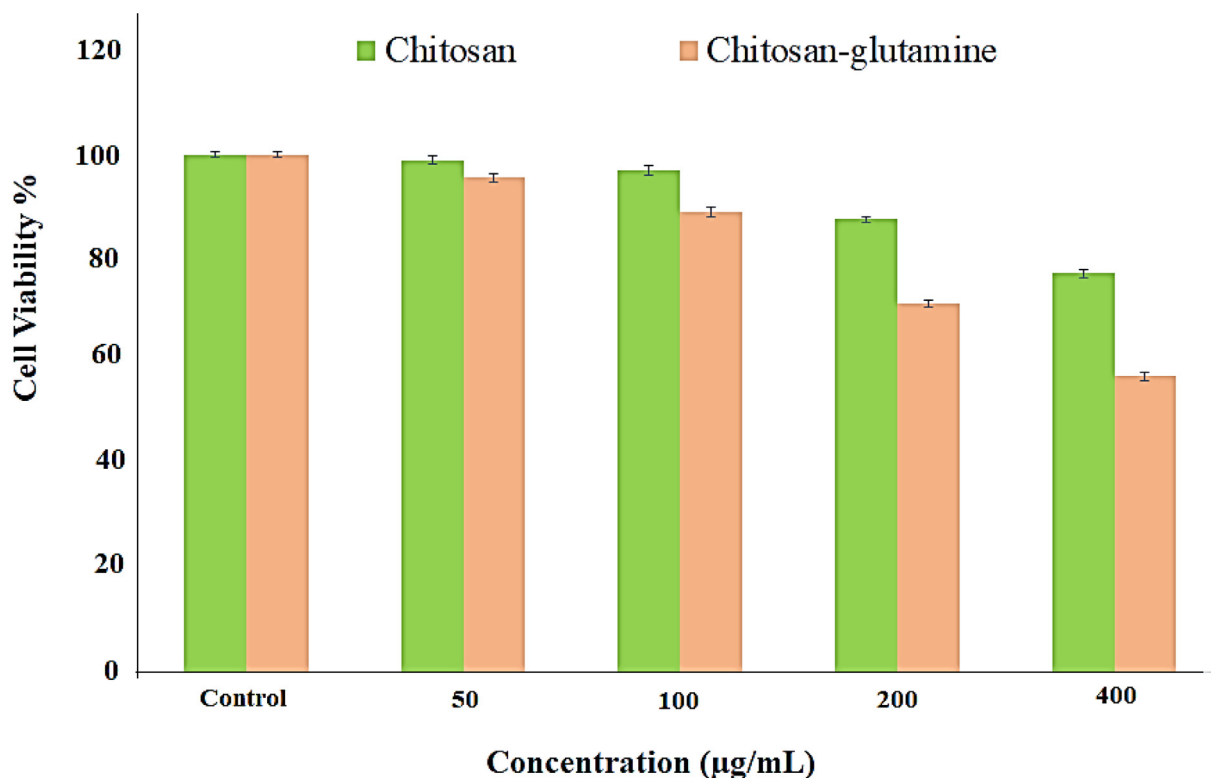

Fig. 8. MTT assay of chitosan and chitosan-glutamine on Hep-G2 cell line after 24 h.

illustrates the chitosan conjugated to glutamine. To confirm the synthesis, the functional groups of the chitosan-glutamine were investigated with FT-IR spectroscopy as shown in Fig. 2. As can be seen several absorption bands are appeared in FT-IR spectra that are corresponding to the main functional groups in chitosan-glutamine structure such as amine (N—H), carbonyl (C═O), hydroxyl groups (O—H), and alkane (C—O, and C—H). Briefly, the absorption band at 3451 cm^{-1} and 946 cm^{-1} are related to the stretching vibration and bending vibrations of the O—H, respectively. The C—H stretching bonds are appeared at 2922 cm^{-1} to 2945 cm^{-1} wavelength that are related to the aliphatic vibration's backbone. The two sharp peak at 1031 cm^{-1} and 1179 cm^{-1} shows the symmetric vibrations of the C—O bond. The stretching vibrations of the C-N bond is observed at 1268 cm^{-1}. Besides, the N—H stretching vibration (amine) is appeared at 3311 cm^{-1} wavelengths, while N—H bending are appeared at 1510 cm^{-1} and 1587 cm^{-1} wavelengths (Fernandes Queiroz et al., 2014, Saber-Samandari et al., 2015). The sharp absorption band at 1693 cm^{-1} is clearly represent the stretching vibration of the C═O bond. Prior investigations involved FT-IR analysis of chitosan and glutamine separately (Drabczyk et al., 2020, Absalan and Noroozi-Shad 2021). By comparing the FT-IR spectrum of the chitosan-glutamine nano-conjugate with the individual spectra of chitosan and glutamine, it was evident that the successful synthesis of the chitosan-glutamine nano-conjugate had been achieved.

Also, ^{1}H NMR spectroscopy performed for determination the structure of chitosan conjugated with glutamine (Fig. 3). The sharp multi-branched signals with an area of 8.70 in the range of 0.9–1.0 ppm are related to the protons of methylene (—CH$_2$—) group in the chitosan chain. The broad signals with area of 2.98 in the range of 2.2 to 2.3 ppm are corresponding to —CH$_2$- protons in the structure of glutamine. The connected protons to oxygen atom in chitosan are appeared as multi-branched signals in the range of 2.8–3.0 ppm. The double weak peak with an area of 2.79 in the range of 3.6 ppm is related to the methylene (—CH$_2$-) protons closed to the hydroxyl group (—OH) in chitosan. Finally, the weak peak with an area of 0.34 at 8.0 ppm is related to the protons of amino groups (—NH$_2$) of chitosan. ^{1}H NMR analyzes showed that
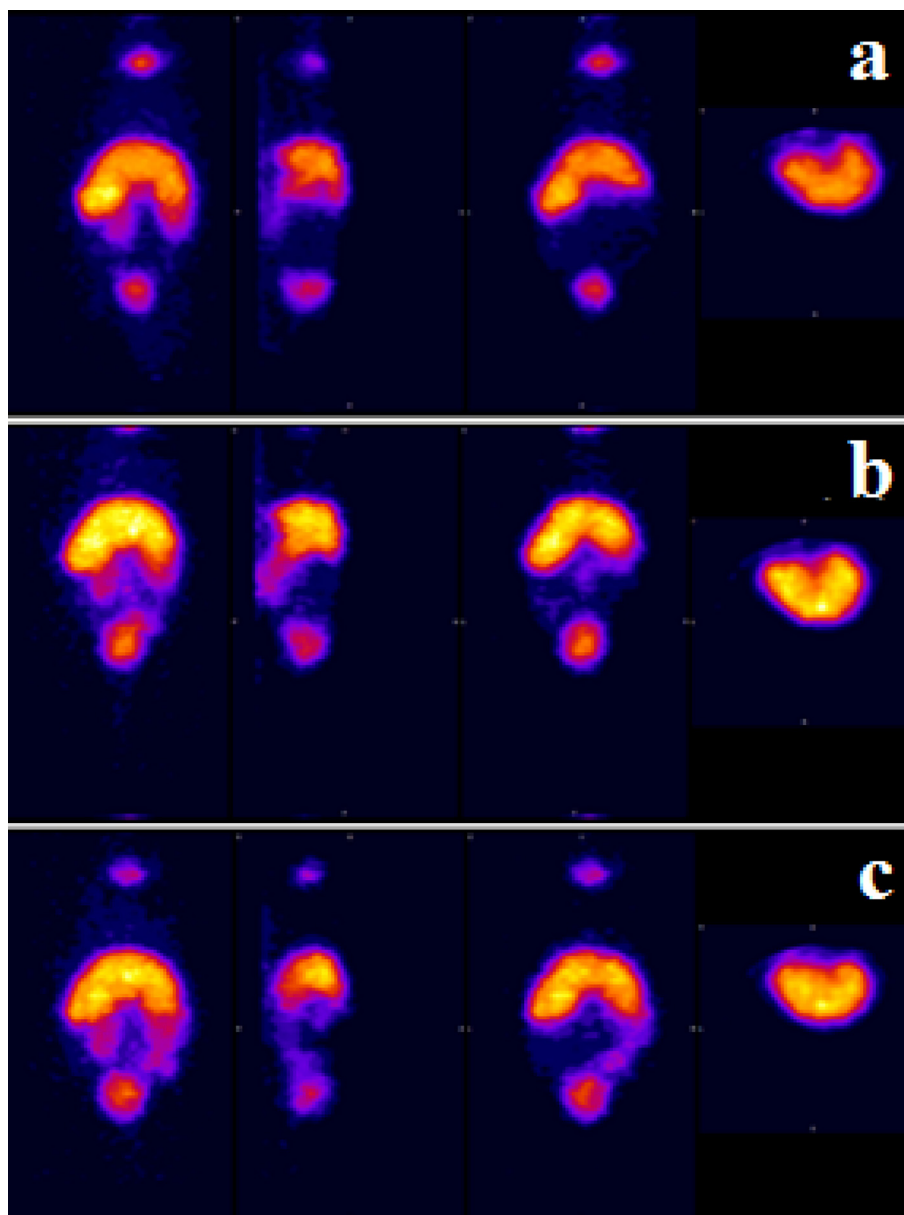

Fig. 9. Whole body SPECT imaging of ^{99m}Tc-chitosan-glutmine in mice (a) 15 min, (b) 60 min and (c) 120 min.

M. Nejati, M.P. Hamedani, Seyed Esmaeil Sadat Ebrahimi et al.

Arabian Journal of Chemistry 16 (2023) 105284

proposed protons are located in the desired position that is clarify the successful preparation of chitosan-glutamine structure (Choi et al., 2015). Moreover, SLS spectroscopy was done for determination of exact molecular weight of the nano-conjugate. Result showed that chitosan-glutamine nano-conjugate had a 28.2 ± 4.17 molecular weight (kD).

Furthermore, the surface morphology of chitosan-glutamine nanoparticles was characterized using FESEM at two different magnification scales of 100 (500 nm) and 200 kX (200 nm). FESEM micrographs in Fig. 4 depict regular particles with a unique distribution at 100 kX magnification. Upon increasing the magnification to 200 kX, the spherical nano-conjugate exhibited a more pronounced and distinct appearance. The nano-conjugate appeared a fairly uniform shape, with noticeable beads present on their surface. The occurrence of clumping in certain areas of the image can be attributed to the particles' reduced surface charge. However, due to the small size of the particles (<100 nm) uncontrollable aggregation was observed. The similar results were reported in previously published works (Tao et al., 2011, Nui Pham et al., 2016). The particle size distribution was analyzed using *ImagJ* software and an average size of 42 nm was determined for chitosan-glutamine nanoparticles. The reduced particle size enhances the porous structure and surface area.

To investigate the particle size distribution, DLS analysis was conducted for chitosan-glutamine nano-conjugate in deionized water. Fig. 5 represents the resulting DLS graph, showing the particles number (per count) versus the particle size (nm). As a result, the DLS analysis predicts a mean value of 100 nm for the measured particle diameter. The surface charge of the nanoparticles was studied based on zeta potential. Herein, Fig. 6 shows the predicted positive surface charges (+9.83 mV) for chitosan-glutamine nano-conjugate.

Moreover, AFM microscopy is a powerful technique to studying the surface of nanoparticles. In two-dimensional micrograph (Fig. 7a) the dark points with low altitude show the depth or valleys, while the brighter point indicates the height of the particles. Particularly, this micrograph is used to display the particle size distribution and does not provide exact height measurements of the particles. Three-dimensional AFM micrograph (Fig. 7b), is displayed at the sample area of 5 μm, the light parts indicate the

height of particles, while the darker parts represent the depth. Difference between the highest and lowest height (peak-to-valley roughness) is obtained 39 nm. The sample roughness index (RMS) is measured for the surface of nanoparticles with value of 6.7 nm. RMS is an important characteristics factor that can affect the surface of nanomaterials by affecting the adhesion force, electron, optical properties, and surface energy. Additionally, by using the AFM microscopy, the measuring of the particle size also possible. Fig. 7c is indicating the average size of nanoparticles around 103 nm.

The cytotoxicity of chitosan-glutamine nano-conjugate was investigated in-vitro on Hep-G_2 cell line using the MTT assay. As shown in Fig. 8, the data clearly demonstrate that nano-conjugate showed higher toxicity on Hep-G_2 cell line compare to chitosan alone. Result showed the significant difference between nano-conjugate at different concentration and control group. For further investigation, an in-vivo study was conducted in mouse model. The chitosan-glutamine was radiolabeled with technetium-99 m and radiochemical purity of labelled nano-conjugate was determined about 90 percent by TLC chromatography. After injection of ^{99m}Tc-chitosan-glutamine (1.4 mCi), mice were anesthetized and placed under the SPECT instrument for imaging at various intervals (15, 60 and 120 min). Fig. 9 illustrates the results, revealing distinct visibility of the liver and spleen by SPECT images. Following SPECT imaging, the mice were scarified and each organ (liver, kidney, lung, heart, brain, spleen, intestine, and bladder) was collected to conduct a biodistribution study measuring the percentage of injected dose per gram (% ID/g). Radioactivity accumulation in each organ was assessed after 120 min and the findings are presented in Fig. 10. The variation in % ID/g values among the organs clearly indicates a significant distinction in accumulation between the liver and other tissues. Therefore, it can be inferred that this radiotracer is well-suited for liver imaging.

All in all, based on the findings from SPECT imaging and biodistribution analysis, it can be concluded that the labeled nano-conjugate possesses the potential to serve as a nano-radiopharmaceutical for liver imaging. Additionally, the MTT assay demonstrated toxicity towards the cancer cell line, suggesting that this nano-radiotracer could potentially be utilized as a theranostic agent for cancer cells.
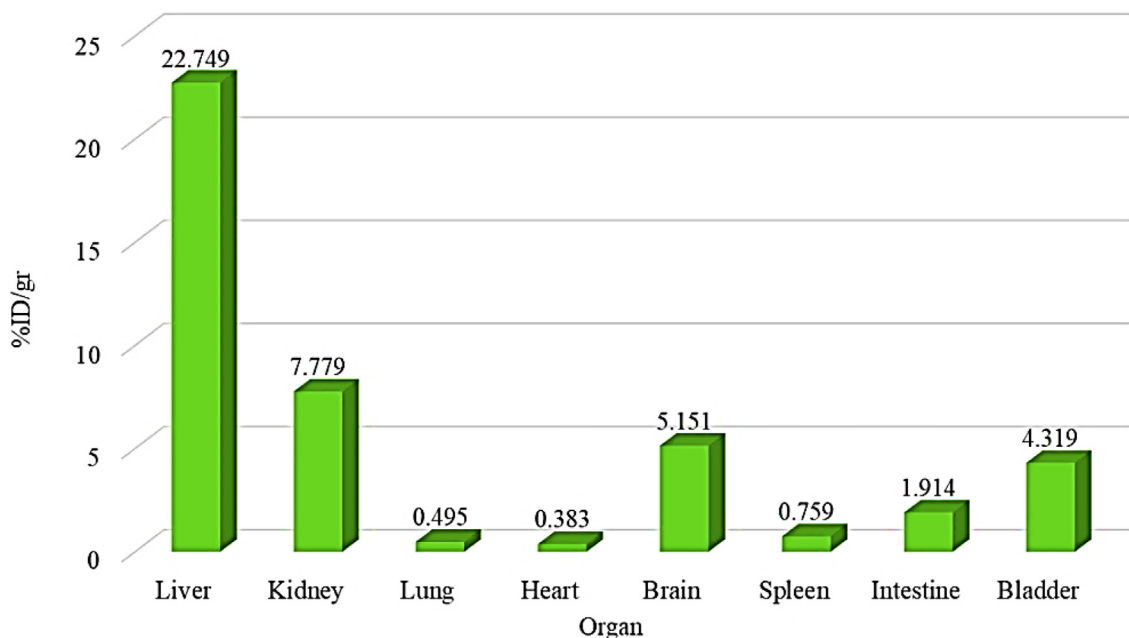

Fig. 10. Percentage of ^{99m}Tc-chitosan-glutmine accumulation in different organs after 120 min.

M. Nejati, M.P. Hamedani, Seyed Esmaeil Sadat Ebrahimi et al.

Arabian Journal of Chemistry 16 (2023) 105284

4. Conclusion

Successful synthesis of chitosan conjugated to glutamine nanoparticle has been clearly confirmed by multitude spectroscopy techniques including FT-IR, ^{1}H NMR, DLS, AFM, and FESEM and nanometer range was confirmed. Chitosan-glutamine nano-conjugate showed the positive surface charge. Profoundly noteworthy, the MTT assay demonstrated that nano-conjugate showed higher toxicity on Hep-G2 cell line compare to chitosan alone. Moreover, SPECT imaging of the labelled chitosan-glutamine nano-conjugate with technetium-99 m showed the suitable accumulation in liver and spleen. Furthermore, the biodistribution result has exhibited significant accumulation of ^{99m}Tc-chitosan-glutamine nano-conjugate in liver compare to other organ. These innovative discoveries, conclusively paramount, signify a promising advancement in the field and warrant further investigation and exploration and suggest that chitosan-glutamine nano-conjugate maybe serve as an alternative nano-radiopharmaceutical for liver imaging in the future.

Declaration of Competing Interest

The authors declare that they have no known competing financial interests or personal relationships that could have appeared to influence the work reported in this paper.

Acknowledgment

References

Absalan, Y., Noroozi-Shad, N., 2021. The Complex compound of amino acids with Titanium (III) as a method to control and synthesis of different structures of TiO₂ nanoparticles; usage as photocatalysts to oxidize alcohols to aldehyde.

Albernaz Mde, S., Ospina, C.A., Rossi, A.M., et al., 2014. Radiolabelled nanohydroxyapatite with 99mTc: perspectives to nanoradiopharmaceuticals construction. Artif. Cells Nanomed. Biotechnol. 42, 88–91. https://doi.org/10.3109/21691401.2013.785954.

Amin, K.C., Saha, G.B., Go, R.T., 1997. A Rapid Chromatographic Method for Quality Control of Technetium-99m-Bicisate. J. Nucl. Med. Technol. 25, 49–51.

Braga, T.L., 2015. Development of nano radiopharmaceutical based on Bevacizumab labelled with Technetium-99m for early diagnosis of gastrointestinal stromal tumor. Available from INIS: http://inis.iaea.org/search/search.aspx?orig_q=RN:46062692.

Cędrowska, E., Pruszynski, M., Majkowska-Pilip, A., et al., 2018. Functionalized TiO(2) nanoparticles labelled with (225)Ac for targeted alpha radionuclide therapy. J. Nanoparticle Res.: An Interdisc. Forum Nanoscale Sci. Technol. 20, 83. https://doi.org/10.1007/s11051-018-4181-y.

Chen, L., Zhong, X., Yi, X., et al., 2015. Radionuclide (131)I labeled reduced graphene oxide for nuclear imaging guided combined radio- and photothermal therapy of cancer. Biomaterials 66, 21–28. https://doi.org/10.1016/j.biomaterials.2015.06.043.

Choi, B., Cui, Z.-K., Kim, S., et al., 2015. Glutamine-chitosan modified calcium phosphate nanoparticles for efficient siRNA delivery and osteogenic differentiation. J. Mater. Chem. B 3, 6448–6455. https://doi.org/10.1039/C5TB00843C.

de Souza Albernaz, M., de Carvalho Patricio, B.F., Weissmuller, G., et al., 2012. Polymeric nanoparticles of FMISO: are nano-radiopharmaceuticals better than conventional ones? Curr. Radiopharm. 5, 336–339. https://doi.org/10.2174/1874471011205040336.

Drabczyk, A., Kudłacik-Kramarczyk, S., Głąb, M., et al., 2020. Physicochemical investigations of chitosan-based hydrogels containing aloe vera designed for biomedical use. Journal 13. https://doi.org/10.3390/ma13143073.

Dunphy, M.P.S., Harding, J.J., Venneti, S., et al., 2018. In vivo PET assay of tumor glutamine flux and metabolism: in-human trial of (18)F-(2S,4R)-4-Fluoroglutamine. Radiology 287, 667–675. https://doi.org/10.1148/radiol.2017162610.

Eberlein, U., Bröer, J.H., Vandevoorde, C., et al., 2011. Biokinetics and dosimetry of commonly used radiopharmaceuticals in diagnostic nuclear medicine - a review. Eur. J. Nucl. Med. Mol. Imaging 38, 2269–2281. https://doi.org/10.1007/s00259-011-1904-z.

Ebrahimzadeh, M.A., Hashemi, Z., Mohammadyan, M., et al., 2021. In vitro cytotoxicity against human cancer cell lines (MCF-7 and AGS), antileishmanial and antibacterial activities of green synthesized silver nanoparticles using Scrophularia striata extract. Surf. Interfaces 23,. https://doi.org/10.1016/j.surfin.2021.100963 100963.

Enrique, M.A., Mariana, O.R., Mirshojaei, S.F., et al., 2015. Multifunctional radiolabeled nanoparticles: strategies and novel classification of radiopharmaceuticals for cancer treatment. J. Drug Target. 23, 191–201. https://doi.org/10.3109/1061186x.2014.988216.

Eroglu, H., Yenilmez, A., 2016. An investigation of the usability of solid lipid nanoparticles radiolabelled with Tc-99m as imaging agents in liver-spleen scintigraphy. J. Biomed. Nanotechnol. 12, 1501–1509. https://doi.org/10.1166/jbn.2016.2286.

Fernandes Queiroz, M., Melo, K.R., Sabry, D.A., et al., 2014. Does the use of chitosan contribute to oxalate kidney stone formation? Mar. Drugs 13, 141–158. https://doi.org/10.3390/md13010141.

Ferro-Flores, G., Ocampo-García, B.E., Santos-Cuevas, C.L., et al., 2015. Theranostic radiopharmaceuticals based on gold nanoparticles labeled with (177)Lu and conjugated to peptides. Curr. Radiopharm. 8, 150–159. https://doi.org/10.2174/1874471008666150313115423.

Ghoreishi, S.M., Khalaj, A., Sabzevari, O., et al., 2018. Technetium-99m chelator-free radiolabeling of specific glutamine tumor imaging nanoprobe: in vitro and in vivo evaluations. Int. J. Nanomed. 13, 4671–4683. https://doi.org/10.2147/ijn.s157426.

Hashemi, Z., Mizwari, Z.M., Mohammadi-Aghdam, S., et al., 2022a. Sustainable green synthesis of silver nanoparticles using Sambucus ebulus phenolic extract (AgNPs@SEE): Optimization and assessment of photocatalytic degradation of methyl orange and their in vitro antibacterial and anticancer activity. Arab. J. Chem. 15,. https://doi.org/10.1016/j.arabjc.2021.103525 103525.

Hashemi, Z., Shirzadi-Ahodashti, M., Mortazavi-Derazkola, S., et al., 2022b. Sustainable biosynthesis of metallic silver nanoparticles using barberry phenolic extract: optimization and evaluation of photocatalytic, in vitro cytotoxicity, and antibacterial activities against multidrug-resistant bacteria. Inorg. Chem. Commun. 139,. https://doi.org/10.1016/j.inoche.2022.109320 109320.

Hjelstuen, O.K., 1995. Technetium-99m chelators in nuclear medicine. A review. Analyst 120, 863–866. https://doi.org/10.1039/AN9952000863.

Hu, Z., Qu, Y., Wang, K., et al., 2015. In vivo nanoparticle-mediated radiopharmaceutical-excited fluorescence molecular imaging. Nat. Commun. 6, 7560. https://doi.org/10.1038/ncomms8560.

Janssen, I., Chen, C.C., Millo, C.M., et al., 2016. PET/CT comparing (68)Ga-DOTATATE and other radiopharmaceuticals and in comparison with CT/MRI for the localization of sporadic metastatic pheochromocytoma and paraganglioma. Eur. J. Nucl. Med. Mol. Imaging 43, 1784–1791. https://doi.org/10.1007/s00259-016-3357-x.

Kakkar, D., Tiwari, A.K., Chuttani, K., et al., 2010. Comparative evaluation of glutamate-sensitive radiopharmaceuticals: Technetium-99m-glutamic acid and technetium-99m-diethylenetriaminepentaacetic acid-bis(glutamate) conjugate for tumor imaging. Cancer Biother. Radiopharm. 25, 645–655. https://doi.org/10.1089/cbr.2010.0848.

Kleynhans, J., Grobler, A.F., Ebenhan, T., et al., 2018. Radiopharmaceutical enhancement by drug delivery systems: a review. J. Control. Release 287, 177–193. https://doi.org/10.1016/j.jconrel.2018.08.008.

Lopci, E., Grassi, I., Chiti, A., et al., 2014. PET radiopharmaceuticals for imaging of tumor hypoxia: a review of the evidence. Am. J. Nucl. Med. Mol. Imaging 4, 365–384.

Nui Pham, X., Phuoc Nguyen, T., Nhung Pham, T., et al., 2016. Synthesis and characterization of chitosan-coated magnetite nanoparticles and their application in curcumin drug delivery. Adv. Nat. Sci. Nanosci. Nanotechnol. 7,. https://doi.org/10.1088/2043-6262/7/4/045010 045010.

Othman, S.H., Ibrahim, I.A., Hatab, M.H., et al., 2016. Preparation, characterization and biodistribution in quails of (99m)Tc-folic acid/chitosan nanostructure. Int. J. Biol. Macromol. 92, 550–560. https://doi.org/10.1016/j.ijbiomac.2016.07.065.

Paul, P., Sengupta, S., Mukherjee, B., et al., 2018. Chitosan-coated nanoparticles enhanced lung pharmacokinetic profile of voriconazole upon pulmonary delivery in mice. Nanomedicine (Lond.) 13, 501–520. https://doi.org/10.2217/nnm-2017-0291.

Rasaneh, S., Johari-Daha, F., 2015. The application of 99mTc-chitosan microparticles in lung imaging of mice: a short report. RUMS_JOURNAL. 13, 1013–1018.

Rudzinski, W.E., Palacios, A., Ahmed, A., et al., 2016. Targeted delivery of small interfering RNA to colon cancer cells using chitosan and PEGylated chitosan nanoparticles. Carbohydr. Polym. 147, 323–332. https://doi.org/10.1016/j.carbpol.2016.04.041.

Saber-Samandari, S., Yekta, H., Saber-Samandari, S., 2015. Effect of iron substitution in hydroxyapatite matrix on swelling properties of composite bead. JOM 9, 19–25.

Sakr, T., Morsy, S., Mahmoud, N., et al., 2018. Preparation, Characterization, Cytotoxicity and Biological Evaluation of <sup>99m</sup>Tc-Doxorubicin-Epigallocatechingallate Functionalized Gold Nanoparticles as a New Generation of Theranostic Radiopharmaceutical, Preprints.org.

Shao, X., Zhang, H., Rajian, J.R., et al., 2011. 125I-labeled gold nanorods for targeted imaging of inflammation. ACS Nano 5, 8967–8973. https://doi.org/10.1021/nn203138t.

Silindir-Gunay, M., Ozer, A.Y., 2017. Chapter 22 - Nanosized drug delivery systems as radiopharmaceuticals. In: Ficai, A., Grumezescu, A.M. (Eds.), Nanostructures for Cancer Therapy. Elsevier, pp. 563–592.

Surasi, D.S., O'Malley, J., Bhambhvani, P., 2015. 99mTc-tilmanocept: a novel molecular agent for lymphatic mapping and sentinel lymph node localization. J. Nucl. Med. Technol. 43, 87–91. https://doi.org/10.2967/jnmt.115.155960.

Taggart, M.P., Tarn, M.D., Esfahani, M.M.N., et al., 2016. Development of radiodetection systems towards miniaturised quality control of PET and SPECT radiopharmaceuticals. Lab Chip 16, 1605–1616. https://doi.org/10.1039/C6LC00099A.

Tao, Y., Zhang, H., Gao, B., et al., 2011. Water-soluble chitosan nanoparticles inhibit hypercholesterolemia induced by feeding a high-fat diet in male Sprague-Dawley rats. J. Nanomater. 2011,. https://doi.org/10.1155/2011/814606 814606.

Unsoy, G., Khodadust, R., Yalcin, S., et al., 2014. Synthesis of Doxorubicin loaded magnetic chitosan nanoparticles for pH responsive targeted drug delivery. Eur. J. Pharm. Sci. 62, 243–250. https://doi.org/10.1016/j.ejps.2014.05.021.

Yhee, J.Y., Song, S., Lee, S.J., et al., 2015. Cancer-targeted MDR-1 siRNA delivery using self-cross-linked glycol chitosan nanoparticles to overcome drug resistance. J. Control. Release 198, 1–9. https://doi.org/10.1016/j.jconrel.2014.11.019.

Zhang, Y., Lv, T., Zhang, H., et al., 2017. Folate and heptamethine cyanine modified chitosan-based nanotheranostics for tumor targeted near-infrared fluorescence imaging and photodynamic therapy. Biomacromolecules 18, 2146–2160. https://doi.org/10.1021/acs.biomac.7b00466.

Zhou, B., Wang, R., Chen, F., et al., 2018. (99m)Tc-Labeled RGD-polyethylenimine conjugates with entrapped gold nanoparticles in the cavities for dual-mode SPECT/CT imaging of hepatic carcinoma. ACS Appl. Mater. Interfaces 10, 6146–6154. https://doi.org/10.1021/acsami.7b17107.